ResearchGate

See discussions, stats, and author profiles for this publication at: https://www.researchgate.net/publication/231632712

Matrix Photochemistry of CH3C(O)SX Molecules with X = H, CH3, and C(O)CH3: Formation of Ketene in Another Decomposition Channel of Sulfenyl Carbonyl Compounds

ARTICLE *in* THE JOURNAL OF PHYSICAL CHEMISTRY A · JULY 2002

Impact Factor: 2.69 · DOI: 10.1021/jp0205261

CITATIONS
36

READS
31

3 AUTHORS:

Rosana Romano
National University of La Plata
116 PUBLICATIONS **863** CITATIONS
SEE PROFILE

Carlos O. Della Vedova
National University of La Plata
293 PUBLICATIONS **2,673** CITATIONS
SEE PROFILE

Anthony J Downs
University of Oxford
258 PUBLICATIONS **5,035** CITATIONS
SEE PROFILE

Available from: Anthony J Downs
Retrieved on: 22 January 2016

Matrix Photochemistry of $CH_3C(O)SX$ Molecules with X = H, CH_3, and $C(O)CH_3$: Formation of Ketene in Another Decomposition Channel of Sulfenyl Carbonyl Compounds

Rosana M. Romano,[‡,†] Carlos O. Della Védova,[‡,§,†] and Anthony J. Downs*[,#]

CEQUINOR (CONICET-UNLP) and Laboratorio de Servicios a la Industria y al Sistema Científico (UNLP-CIC-CONICET), Departamento de Química, Facultad de Ciencias Exactas, Universidad Nacional de La Plata, 47 esq. 115, (1900) La Plata, Argentina, and Inorganic Chemistry Laboratory, University of Oxford, South Parks Road, Oxford OX1 3QR, U.K.

Received: February 26, 2002; In Final Form: April 18, 2002

$CH_3C(O)SC(O)CH_3$ isolated in solid Ar, N_2, or 5% CO-doped Ar at 15 K and $CH_3C(O)SH$ and $CH_3C(O)SCH_3$ isolated in solid Ar at 15 K were irradiated with broad-band UV−visible light ($200 \leq \lambda \leq 800$ nm). On the basis of the IR spectra of the matrixes, hydrogen abstraction from the CH_3 group to give ketene, $H_2C{=}C{=}O$, with the elimination of HX [X = $SC(O)CH_3$, SH, or SCH_3] was identified in each case as the main channel of photodecomposition within the confines of a solid matrix environment. The presence of a CH_3 ligand attached to the carbonyl function thus introduces a third type of elimination reaction for matrix-isolated sulfenyl carbonyl compounds of the general type XC(O)SY. Additionally, the conformational properties of the $CH_3C(O)SX$ molecules have been investigated. In the case of thioacetic acid (X = H), the matrix experiments indicate that the vapor at ambient temperatures consists of a mixture of the syn and anti forms, with the syn form predominating (ca. 85%). Broad-band UV−visible irradiation then results in interconversion of the conformers prior to decomposition. The identification of the different molecules has been underpinned by the results of ab initio and density functional theory (DFT) calculations.

Introduction

The matrix photochemistries of several sulfenyl carbonyl compounds have been investigated[1−4] to reveal some notable properties relating not only to conformational preferences and changes but also to the products of photodecomposition. Molecules containing the −C(O)S− moiety have two potential energy minima corresponding to the syn and anti conformers (eq 1). Although the relative stabilities of the two forms depend

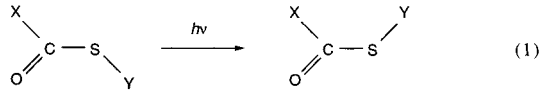

(1)

syn anti

on the compound, the syn conformer is always favored over the anti one.[3,5−7] Broad-band UV−visible irradiation of the matrix-isolated compounds has then been shown to result in a randomization process. For molecules such as FC(O)SCl[4] and FC(O)SBr[3] that display a conformational equilibrium at ambient temperature, the IR bands corresponding to the anti form are observed to grow at the expense of those due to the syn form until an approximately equimolar mixture of the two forms develops. For molecules that exist effectively as a single conformer at ambient temperatures, for example, ClC(O)SBr[1] and $FC(O)SCH_3$,[8] photolysis may nevertheless induce the formation of the anti form.

In addition to these conformational features, the photodecomposition brought about by continued broad-band UV−visible irradiation of the matrix-isolated sulfenyl carbonyl compound affords a convenient means of generating novel species, which are generally short-lived under normal conditions. Thus, one of the common decomposition channels open to a molecule of the type XC(O)SY under matrix conditions leads to the formation of XSY and CO, and the sulfur dihalides ClSF,[2] BrSF[3] and BrSCl[1] can be educed in this way. A second channel results in the elimination of OCS with the formation of XY.[1]

More recently, the structure and conformational properties of diacetyl sulfide, $CH_3C(O)SC(O)CH_3$, in the gaseous and solid phases have been determined.[9] Different experimental and theoretical methods (gas electron diffraction, single-crystal X-ray diffraction, vibrational spectroscopy, and both ab initio and density functional theory methods) reveal that the molecule exists predominantly as a single conformer with a planar heavy-atom skeleton adopting an [sp,ap] configuration.

In this context, the matrix photochemistry of diacetyl sulfide invites investigation not only to seek possible higher energy conformations but also to determine the mode of its decomposition. Here, we report the results of such studies with diacetyl sulfide isolated in solid Ar, N_2, or CO-doped Ar matrixes at ca. 15 K. Although broad-band UV−visible irradiation gave no positive sign of other conformers, the compound was found to have a very rich photochemistry, giving rise to several products issuing from different decomposition channels. To help interpret the results, similar studies were also carried out on two simpler compounds containing the $CH_3C(O)S-$ fragment, namely, $CH_3C(O)SH$ and $CH_3C(O)SCH_3$.

In contrast with diacetyl sulfide, these last two compounds have not been investigated hitherto with regard to either their conformational properties or photodecomposition. The structure

* To whom correspondence should be addressed.
‡ CEQUINOR (CONICET-UNLP), Universidad Nacional de La Plata.
† Member of the Carrera del Investigador Científico del Consejo Nacional de Investigaciones Científicas y Técnicas, República Argentina.
§ Laboratorio de Servicios a la Industria y al Sistema Científico (UNLP-CIC-CONICET), Universidad Nacional de La Plata.
# University of Oxford.

10.1021/jp0205261 CCC: $22.00 © 2002 American Chemical Society
Published on Web 07/12/2002

of the gaseous thioacetic acid molecule has been investigated on the basis of its electron-diffraction pattern,[10] but only the C═O, C−S, and C−C distances and the CCO and CCS angles could be estimated. So low is the scattering power of hydrogen that such measurements are quite insensitive to the orientation of the S−H bond and fail therefore to distinguish between syn and anti conformations of the molecule. The structures of the related compounds $CF_3C(O)SH$ and $CF_3C(O)SCH_3$ have been investigated both theoretically and by gas electron diffraction (GED) methods.[11] Calculations at various levels of theory predict that the syn conformation of $CF_3C(O)SH$ is 0.9−2.2 kcal mol^{-1} more stable than the anti one, and the GED pattern could be accounted for perfectly satisfactorily with a model that involves only the syn form. Likewise with $CF_3C(O)SCH_3$, it is the syn conformer that predominates.

Experimental Section

Commercial samples (Aldrich) of thioacetic acid, $CH_3C(O)SH$ (**1**), and methyl thioacetate, $CH_3C(O)SCH_3$ (**2**), were purified by repeated trap-to-trap condensation in vacuo, and the purity of each was checked by reference to the IR spectrum of the vapor. Diacetyl sulfide, $CH_3C(O)SC(O)CH_3$ (**3**), was prepared by the reaction of thioacetic acid, $CH_3C(O)SH$, with $CH_3C(O)Cl$, according to the published procedure.[12] The compound was isolated by distillation at low pressure and subsequently purified by repeated trap-to-trap condensation in vacuo until it appeared colorless. Its purity was checked by reference to its IR, Raman, and ^1H and ^{13}C NMR spectra.[13] The matrix gases, Ar, N_2, and CO (all BOC, research grade), were used as supplied.

Gas mixtures of **1** and **2** with Ar and of **3** with Ar, N_2, and Ar doped with 5% CO with approximate compositions **X**/matrix gas = 1:1000 (**X** = **1**, **2**, or **3**) were prepared by standard manometric methods. Each such mixture was deposited on a CsI window cooled to ca. 15 K by a Displex closed-cycle refrigerator (Air Products, model CS202) using the pulsed deposition technique.[14,15] The IR spectrum of each matrix sample was recorded at a resolution of 0.5 cm^{-1} and with 256 scans using a Nicolet Magna-IR 560 FTIR instrument equipped with either an MCTB or a DTGS detector (for the ranges 4000−400 cm^{-1} or 600−250 cm^{-1}, respectively). Following deposition and IR analysis of the resulting matrix, the sample was exposed to broad-band UV−visible radiation ($200 \leq \lambda \leq 800$ nm) from a Spectral Energy Hg−Xe arc lamp operating at 800 W. The output from the lamp was limited by a water filter to absorb infrared radiation and so minimize any heating effects. The IR spectrum of the matrix was then recorded at different times of irradiation to scrutinize closely the decay and growth of the various absorptions. Experiments were also performed with a filter cutting out visible light and so confining the photolyzing radiation to wavelengths in the range 200−400 nm. The only difference observed was a uniform diminution in the rates of all of the changes brought about with broad-band UV−visible light.

All of the calculations were performed using the Gaussian 98 program system[16] under the Linda parallel execution environment using two coupled personal computers. Different ab initio and density functional theory (DFT) methods were used, in combination with different basis sets. The geometry optimizations were performed using standard gradient techniques by simultaneous relaxation of all of the geometrical parameters. The calculated vibrational properties corresponded in all cases to potential energy minima for which no imaginary frequency was found.

Results and Discussion

To facilitate the interpretation, we will describe the results of experiments involving first the simplest molecule, $CH_3C(O)SH$ (**1**), then proceeding through $CH_3C(O)SCH_3$ (**2**) to the most complicated molecule, $CH_3C(O)SC(O)CH_3$ **(3)**.

(i) $CH_3C(O)SH$, 1. *Conformational Properties*. The IR spectrum of the thioacetic acid molecule, $CH_3C(O)SH$ (**1**), isolated in a solid inert gas at low temperatures has not been described previously. Table 1 presents the wavenumbers and intensities of the IR absorptions observed for a sample of the compound isolated in an Ar matrix at ca. 15 K. Details of the IR spectrum of the vapor, as reported previously,[17] are included for comparison. The new results are consistent with the earlier ones, while revealing significantly more detail.

In fact, several studies of the vibrational spectra of **1** have been carried out previously, often with the aim of seeking evidence of a possible equilibrium between the thiol and thion tautomers.[17−24] However, none of them considered a possible equilibrium between the syn and anti conformers of the $CH_3C(O)SH$ molecule. The matrix-isolation technique is especially well suited to the study of such an equilibrium by virtue of the sharpness of the IR absorptions and the quenching of any conformational interconversion.[1] Indeed, the IR spectrum that we have measured for the matrix-isolated compound does suggest the presence of more than one conformer, the syn form with the S−H bond cis to the C═O bond being accompanied by a small proportion of the anti form with the S−H bond trans to the C═O bond. Moreover, exposure of the matrix to broad-band UV−visible light ($200 \leq \lambda \leq 800$ nm) resulted in growth of the absorptions associated with the second conformer at the expense of those associated with the syn form (eq 2). For

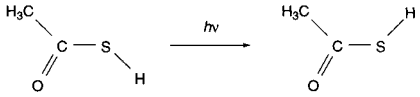

(2)

investigation of the conformational properties of sulfenyl carbonyl compounds, there are few reporters more sensitive to conformation than the ν(CO) fundamental.[1] Figure 1 shows the ν(CO) region of the IR spectrum of **1** (1700−1750 cm^{-1}) at different irradiation times. The most plausible interpretation is that the intense band near 1722 cm^{-1} corresponds to the more stable syn form, while the weaker band near 1729 cm^{-1}, which gains intensity relative to the former on irradiation, corresponds to the anti conformer.

To check this interpretation, we performed ab initio (HF and MP2) and DFT (B3LYP) calculations using a 6-31+G* basis set. The relative stabilities of the two conformers estimated by the different theoretical models are presented in Table 2. The calculated optimum structures are found in all cases to define minima over the potential energy surfaces with no imaginary wavenumbers, and the syn form is invariably more stable than the anti one. On the basis of the theoretical thermodynamic functions, the percentages of each conformer have also been calculated, with the results included in Table 2. Experimental estimates of these percentages could be made by reference to the relative intensities of the corresponding IR absorptions. Thus, the relative intensities of the ν(CO) bands in the spectrum of the initial deposit imply that approximately 18% of the anti form is present in the vapor at ambient temperature, if the ν(CO) modes of the two conformers are assumed to have the same absorption coefficients. If another pair of absorption bands is chosen, the result is slightly different. For example, the relative intensities of the two features near 620 cm^{-1} associated with

TABLE 1: IR Spectra of $CH_3C(O)SH$, 1

Ar matrix		B3LYP/6−31+G* *syn*-$CH_3C(O)SH$		B3LYP/6−31+G* *anti*-$CH_3C(O)SH$			
ν [cm^{-1}]	$I^{b,c}$	ν [cm^{-1}]	$I^{c,d}$	ν [cm^{-1}]	$I^{c,d}$	vapor[a]	assignment[e]
3444[f]							$2\nu(C{=}O_{anti})$
3432						3380	$2\nu(C{=}O_{syn})$
3020.6	0.050 (2)	3163.5	4.8 (1)	3161.9	6.3 (2)	3020	$\nu_a(CH_3)$
2986.2	0.025 (1)	3127.2	3.8 (1)	3125.3	3.8 (1)		$\nu_a(CH_3)$
		3059.3	1.3 (<1)	3059.1	2.2 (<1)	2940	$\nu_s(CH_3)$
2606.5	0.134 (4)	2703.9	1.0 (<1)	2684.2	12.6 (4)	2585	ν(S−H)
2049.6	0.004 (<1)						OCS
1749.2	0.711 (23)						$\nu(C{-}C) + \nu(C{-}S)$
1728.7	0.537 (18)			1796.2	343.6 (100)		$\nu(C{=}O_{anti})$
1722.5	3.045 (100)	1794.6	322.1 (100)			1735	$\nu(C{=}O_{syn})$
1441.2 1435.5	0.163 (5)	1497.9	13.3 (4)	1498.1	15.4 (4)		$\delta_a(CH_3)$
1426.6	0.022 (<1)			1490.0	12.4 (4)		$\delta_a(CH_{3,anti})$
1422.2	0.455 (15)	1487.3	16.8 (5)			1425	$\delta_a(CH_{3,syn})$
1355.2	0.372 (12)	1402.0	23.8 (7)			1365	$\delta_s(CH_{3,syn})$
1353.0	0.035 (1)			1408.3	20.7 (6)		$\delta_s(CH_{3,anti})$
1126.6	2.976 (98)	1147.8	153.9 (48)	1151.6	150.7 (44)	1128	ν(C−C)
1056.6	0.064 (2)	1042.1	3.5 (1)	1042.1	0.7 (<1)	1072	$\rho(CH_3)$
987.2	0.042 (1)			1010.7	29.2 (8)		$\rho(CH_{3,anti})$
983.6	0.548 (18)	1016.7	37.4 (10)			1000	$\rho(CH_{3,syn})$
821.8 819.9 814.4	0.340 (11)	851.5	30.1 (9)	853.1	23.9 (7)	830	δ(CSH)
624.5	0.102 (3)			624.3	69.5 (20)		$\nu(C{-}S_{anti})$
617.3 614.7	1.291 (42)	620.6	81.6 (25)				$\nu(C{-}S_{syn})$
		522.7	2.3 (<1)	531.5	<0.1 (<1)		γ(CO)
445.4	0.035 (1)	444.3	3.3 (1)				$\delta(OSC_{syn})$
427.6				426.5	5.8 (2)		$\delta(OSC_{anti})$
350.7	0.147 (5)	369.5	21.3 (7)	336.9	0.1 (<1)		τ(HSCO)
		322.9	5.8 (2)	316.5	14.6 (4)		δ(CCS)
		45.5	0.1 (<1)	102.1	0.1 (<1)		τ

[a] Reference 17. [b] Intensities in absorbance. [c] Intensities in parentheses normalized relative to that of the most intense band set equal to 100. [d] Intensities in km mol^{-1}. [e] a = antisymmetric, s = symmetric. [f] Visible after irradiation.

the ν(CS) fundamentals would suggest a significantly smaller percentage of the anti conformer (ca. 7%). These results are broadly consistent, however, with the ratios of the absorption coefficients calculated by theory to be 1.07:1 for the ν(CO) bands [anti-ν(CO)/syn-ν(CO)] and 0.85:1 for the ν(CS) bands [again anti-ν(CS)/syn-ν(CS)]. Thus, experiment and theory are more or less agreed about the relative stabilities of the syn and anti forms, with the latter comprising about 16% of the vapor species at room temperature. Moreover, there is also good agreement with the experimental results of Noe[25] for an acetone-d_6 solution of **1**, the temperature dependence of the ^{1}H NMR spectrum indicating a free energy difference of 1.9 kcal mol^{-1} between the two conformers at 17 °C. Although none of the previously reported vibrational studies of **1** take account of this conformational equilibrium, inspection of the IR spectra of the vapor measured by Mecke et al.[19] at 25, 75, and 100 °C reveals the presence and temperature growth of a second ν(CO) band to higher wavenumber of the principal band. This too is completely consistent with the results of our experiments.

The calculated (B3LYP/6-31+G*) wavenumbers and IR intensities for the syn and anti conformers of **1** are included in Table 1 together with the experimental data. All of the IR absorptions anticipated for the anti form by the theoretical calculations can be observed in the spectrum immediately after deposition of the matrix and were seen to grow on broad-band UV−visible irradiation. The theoretical wavenumber shifts of the bands of the anti form relative to those of the syn form are also in good agreement with the experimental ones.

Photochemistry. The matrix doped with **1** was exposed to broad-band UV−visible radiation ($200 \leq \lambda \leq 800$ nm) for different times ranging from 1 to 240 min, and the IR spectrum was measured at each stage. In addition to the conformational interconversion mentioned in the preceding section, several new IR bands appeared and grew at the expense of these due to **1** with progressive photolysis. Attempts to distinguish different products on the basis of the behavior of their IR bands as a function of irradiation time showed only that all of the new bands exhibited the same pattern of growth. The most intense of the new bands, occurring close to 2138 cm^{-1}, suggests at first the presence of the CO molecule invariably formed, it seems, by photodecay of matrix-isolated sulfenyl carbonyl compounds.[1,2,26,27] This feature, attributable to the $\nu(^{12}CO)$ fundamental, is always accompanied by a satellite near 2092 cm^{-1} corresponding to $\nu(^{13}CO)$ with an intensity reflecting the natural abundances of ^{12}C and ^{13}C (ca. 100:1).[27] In the present case, there is indeed a band with an intensity exactly 1% that of the 2138 cm^{-1} band, but it appears near 2082 cm^{-1}, that is, about 10 cm^{-1} to low wavenumber of where the $\nu(^{13}CO)$ mode of free CO would be expected to appear. This finding suggests the development of absorptions coincidentally very close to $\nu(^{12}CO)$ and $\nu(^{13}CO)$ of free CO but belonging to another product. Taking into account not only the 2082 cm^{-1} absorption but also other absorptions near 3061, 1375, 579, and 525 cm^{-1} that appeared after irradiation of the matrix, we are led to conclude that a major photostable product is the ketene molecule, $H_2C{=}C{=}O$ (see Figure 2).[28] In addition to the fundamental vibrational modes, four nonfundamental transitions were also located near 3506, 3249, 3103, and 1945 cm^{-1}. The identity of the product is confirmed by comparison with the IR spectrum reported earlier by Bandow and Akimoto[29] for a solid

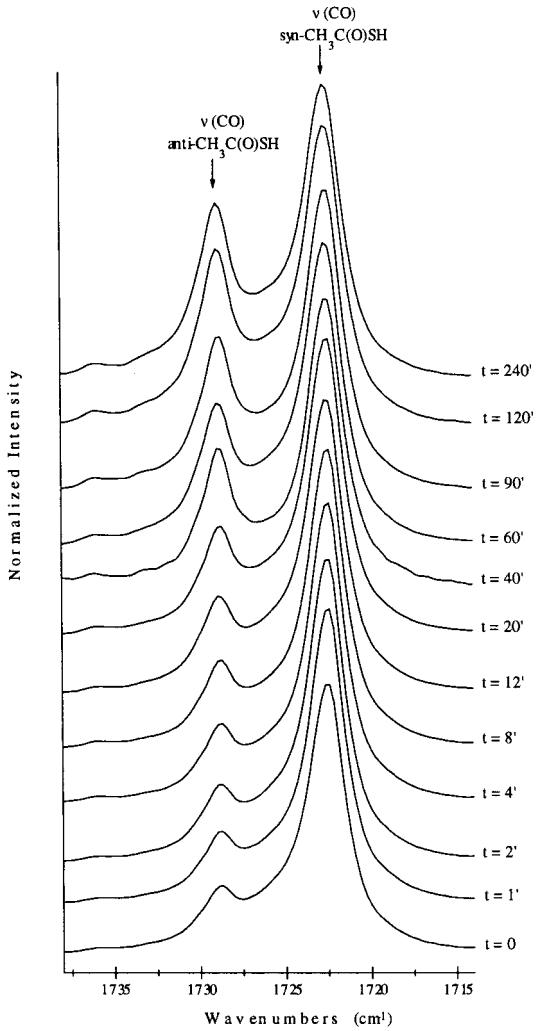

Figure 1. ν(CO) region of the IR spectra of an Ar matrix containing $CH_3C(O)SH$ at different irradiation times.

TABLE 2: Relative Stabilities of the syn and anti Forms of $CH_3C(O)SH$, 1, Calculated with Different Theoretical Models

theoretical model	E_{syn} [hartree]	E_{anti} [hartree]	ΔE [kcal mol^{-1}]	% syn	% anti
HF/6-31+G*	−550.444 071 112	−550.441 141 667	1.84	79	21
B3LYP/6-31+G*	−552.044 930 163	−552.041 963 714	1.86	80	20
MP2/6-31+G*	−551.006 979 2	−551.003 191 2	2.38	85	15

Ar matrix doped with ketene. The previous study also demonstrated the photostability of ketene under these conditions, at least with respect to near-UV light ($310 \leq \lambda \leq 410$ nm).

The formation of ketene suggests that H_2S is eliminated from **1** under the action of broad-band UV−visible light in accordance with eq 3. Figure 3 reproduces the IR spectrum of the matrix

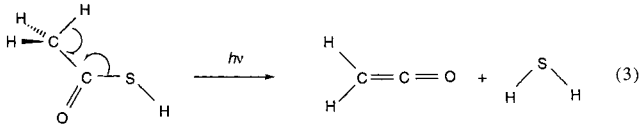

(3)

in the region 2570−2650 cm^{-1} characteristic of ν(SH) modes after 4 h irradiation. In addition to the 2606.5 cm^{-1} band arising from the ν(SH) fundamental of *syn*-$CH_3C(O)SH$, at least four new absorptions appeared at 2630.9, 2620.9, 2617.6, and 2574.8 cm^{-1}. There have been several previous studies of H_2S isolated in different matrix environments.[30,31] These have shown that

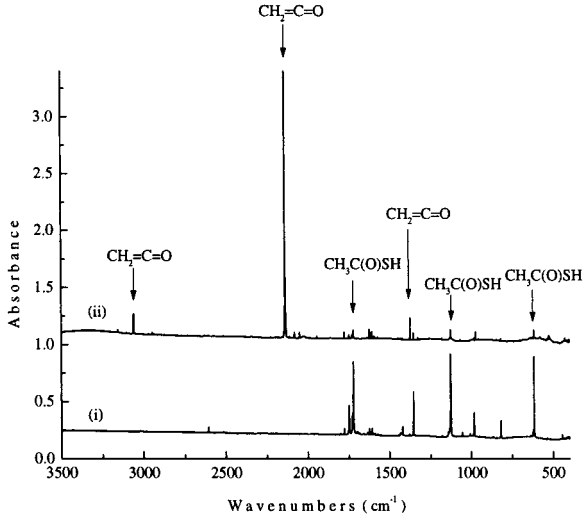

Figure 2. IR spectra of an Ar matrix containing $CH_3C(O)SH$: (i) following deposition and (ii) after 240 min of broad-band UV−visible photolysis.

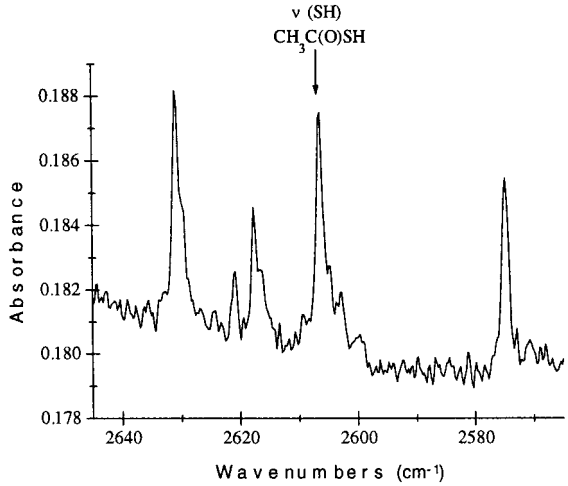

Figure 3. ν(SH) region of the IR spectrum of an Ar matrix initially containing $CH_3C(O)SH$ after 240 min of broad-band UV−visible irradiation.

the wavenumbers and relative intensities of the antisymmetric and symmetric $\nu(SH_2)$ modes exhibit large variations with the switches from the gas to the matrix phase or indeed from one matrix to another.[30] Hence, it appears that the H_2S molecule is highly sensitive to its environment. There is a further potential complication from aggregation to give H_2S multimers, $[H_2S]_n$.[30,32] Moreover, earlier photolysis studies concluded that matrix-bound H_2S decomposes to give HS radicals and S atoms.[32] In light of these factors, the most likely explanation of the new bands shown in Figure 3 is that they arise from the $\nu(SH_2)$ fundamentals of H_2S in different matrix cages, at least some of which also host the ketene molecule.

In addition to the bands attributable to the formation of ketene and H_2S, photolysis resulted in the development of other weak absorptions, as listed in Table 3. We identify these bands with the formation of CH_3SH, OCS, and CH_4 on the basis of the IR spectra reported elsewhere[1,33−35] for authentic samples of each of these molecules in the matrix-isolated state. Hence, it is apparent that H_2S-elimination, as in eq 3, is not the only channel open to the photodecomposition of matrix-isolated **1**. The two pathways represented by eqs 4 and 5 are likely to account for the presence of these compounds (as well as CO, the absorption of which was overlaid presumably by that of ketene); all build

TABLE 3: Wavenumbers, Intensities, and Assignments of the IR Absorptions Appearing after 240 min of Broad-Band Photolysis of $CH_3C(O)SH$ Isolated in an Ar Matrix

IR		assignment		wavenumber reported previously
ν [cm^{-1}]	I	molecule	vibrational mode	
3506.3	0.029	$H_2C{=}C{=}O$	$\nu(C{=}O) + \delta(CH_2)$	3513[a]
3248.9	0.022	$H_2C{=}C{=}O$	$\nu(C{=}O) + \nu(C{-}C)$	3255[a]
3155.9	0.064	$H_2C{=}C{=}O$	$\nu_a(CH_2)$	3155[a]
3103.3	0.017	$H_2C{=}C{=}O$	$\nu(C{=}O) + \rho(CH_2)$ in-plane	
3063.3 3061.1	0.284	$H_2C{=}C{=}O$	$\nu_s(CH_2)$	3062[a]
3046.1	0.009	CH_4	$\nu_a(CH_3)$	3037.0[b]
3008.2 3002.8	0.006	CH_3SH	$\nu_a(CH_3)$	3011.9 3006.4 [c]
2947.0 2935.9	0.046	CH_3SH	$\nu_s(CH_3)$	2948.4 2935.9 [c]
2630.9	0.016	H_2S?		
2620.9	0.002	H_2S?		
2617.6	0.009	H_2S?		
2603.0	<0.002	CH_3SH	$\nu(S{-}H)$	2604.2[c]
2574.8 2572.9	0.010	H_2S?		
2138.2 2134.6	4.476	$H_2C{=}C{=}O$	$\nu(C{=}O)$	2142[a]
2081.8	0.042	$H_2C{=}C{=}O$	$\nu(^{13}C{=}O)$	2085[a]
2049.6	0.059	OCS	$\nu(C{=}O)$	2049.3[d]
1945.3	0.022	$H_2C{=}C{=}O$	$2\rho(CH_2)$ in-plane	1947[a]
1375.0	0.151	$H_2C{=}C{=}O$	$\delta(CH_2)$	1381[a]
1326.3	0.008	CH_3SH	$\delta_s(CH_3)$	1326.5[c]
1304.5	0.009	CH_4	$\delta_s(CH_3)$	1307.7[b]
1068.5	0.014	CH_3SH	$\rho(CH_3)$	1068.2[c]
974.0	0.057	$H_2C{=}C{=}O$	$\rho(CH_2)$ in-plane	974[a]
957.0	0.010	CH_3SH	$\rho(CH_3)$	954.3[c]
799.3	0.003	CH_3SH	$\delta(CSH)$	800.0[c]
703.8	0.004	CH_3SH	$\nu(C{-}S)$	704.3[c]
579.2	0.133	$H_2C{=}C{=}O$	$\rho(CH_2)$ out-of-plane	591[a]
525.3	0.656	$H_2C{=}C{=}O$	$\delta(CO)$ out-of-plane	525[a]
427.6	0.032	$H_2C{=}C{=}O$	$\delta(CCO)$	438[a]

[a] Reference 28. [b] Reference 35. [c] Reference 33. [d] Reference 34.

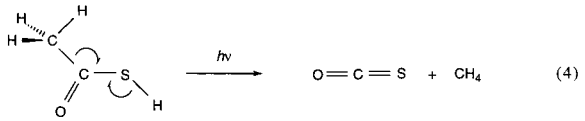

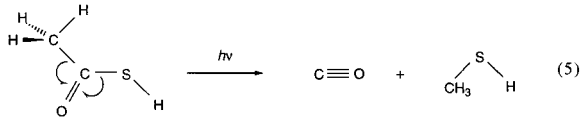

up at the same rate as ketene and H_2S, albeit in smaller yield. Both find clear precedents, for example, in the matrix photochemistry of ClC(O)SBr.[1]

(ii) $CH_3C(O)SCH_3$, 2. *Conformational Properties.* The structure and conformational properties of methyl thioacetate, $CH_3C(O)SCH_3$ (**2**), have not been determined experimentally. To investigate the existence and relative stabilities of different conformers as an aid to the interpretation of the IR spectrum of the matrix-isolated molecule and of the effects of subsequent broad-band UV−visible photolysis, a theoretical study becomes a necessary requirement. For **2**, we also found two minima over the potential energy surface, namely, the syn and anti forms, but the energy difference between the two conformers is now found to be ca. 5 kcal mol^{-1} (see Table 4), a value too high to admit the detection of a significant fraction of the less stable (anti) conformer in the vapor at ambient temperatures.

The IR spectrum of **2** isolated in a solid Ar matrix detailed in Table 5 is entirely consistent with these theoretical results,

TABLE 4: Relative Stabilities of the syn and anti Forms of $CH_3C(O)SCH_3$, 2, Calculated with Different Theoretical Models

theoretical model	E_{syn} [hartree]	E_{anti} [hartree]	ΔE [kcal mol^{-1}]
HF/6-31+G*	−589.481 899 916	−589.474 148 213	4.86
B3LYP/6-31+G*	−591.364 323 625	−591.357 009 192	4.59
MP2/6-31+G*	−590.179 866 1	−590.171 628 3	5.17

TABLE 5: IR Spectra of $CH_3C(O)SCH_3$, 2

Ar matrix		B3LYP/6-31+G* syn-$CH_3C(O)SCH_3$		Ar matrix[a]	
ν [cm^{-1}]	$I^{b,c}$	ν [cm^{-1}]	$I^{c,d}$	ν [cm^{-1}]	assignment[e]
3389.9	0.068 (<1)				2ν(C=O)
		3171.8	2.7 (<1)		
		3169.8	3.3 (1)		
3013.4 3004.9 2993.1	0.350 (4)	3149.5	8.2 (3)	2988	$\nu_a CH_3{-}(C)$)
		3129.0	3.1 (1)	2975	$\nu_a(CH_3{-}(S))$
2938.1	0.445 (5)	3078.7	15.2 (5)	2921	$\nu_s(CH_3{-}(C))$
		3059.8	2.7 (<1)		
1709.3 1701.6	8.474 (100)	1764.6	278.5 (100)	1703	ν(C=O)
		1496.9	13.4 (5)	1430	$\delta_a(CH_3{-}(C))$
1432.5 1428.3	1.313 (15)	1494.9	9.0 (3)		
		1492.0	9.8 (4)	1425	$\delta_a(CH_3{-}(S))$
		1484.6	9.4 (3)		
1355.9	0.470 (6)	1410.7	18.7 (7)	1357 1352	$\delta_s(CH_3{-}(C))$
1309.2	0.118 (1)	1381.6	2.3 (<1)	1304 1302	$\delta_s(CH_3{-}(S))$
1131.5	3.773 (45)	1139.4	152.7 (55)	1126	ν(C−C)
		1030.4	3.1 (1)		
1096.6	1.722 (20)	1020.6	30.9 (11)	1090	$\rho(CH_3{-}(S))$
1004.5 986.5 979.0 974.8 962.9	1.769 (21)	991.4	2.5 (<1)	976 984	$\rho(CH_3{-}(C))$
946.8 939.2	0.514 (6)	969.6	39.5 (14)	948 943	$\rho(CH_3{-}(S))$
725.6	0.088 (1)	718.0	2.8 (1)	724	$\nu(S{-}CH_3)$
627.9 623.6 618.1	1.948 (23)	619.5	59.9 (22)	614	ν(C(O)−S)
532.1 528.8	0.063 (<1)	537.8	1.4 (<1)		δ(OSC)
474.1	0.006 (<1)	486.2	0.7 (<1)	~430	γ(C=O)
360.6	0.111 (1)	353.7	3.8 (1)		δ(CCS)
		207.0	7.6 (3)		δ(CSC)
		132.6	5.4 (2)		τ
		77.0	<0.1 (<1)		τ
		14.2	2.0 (<1)		τ

[a] Reference 36. [b] Intensities in absorbance. [c] Intensities in parentheses normalized relative to that of the most intense band set equal to 100. [d] Intensities in km mol^{-1}. [e] a = antisymmetric, s = symmetric.

affording no sign of the anti form. However, a new band appearing near 1704 cm^{-1} after broad-band UV−visible photolysis of the matrix suggests the formation of the anti conformer under these conditions. The theoretical wavenumber shift of approximately 4 cm^{-1} in the ν(CO) mode with the change from the syn to the anti form is in good agreement with the 3 cm^{-1} shift observed for the new band with respect to the ν(CO) absorption of the syn conformer. Unfortunately, the close similarity between the calculated IR spectra of the two conformers must then be presumed to preclude the observation of any other distinct absorptions attributable to the anti form, but in the circumstances, we cannot rule out the possibility that the

TABLE 6: Wavenumbers, Intensities, and Assignments of the IR Absorptions Appearing after 60 min of Broad-Band Photolysis of $CH_3C(O)SCH_3$ Isolated in an Ar Matrix

IR		assignment		wavenumber reported previously
ν [cm^{-1}]	I	molecule	vibrational mode	
3505.0	0.022	$H_2C{=}C{=}O$	ν(C=O) + $\delta(CH_2)$	3513[a]
3154.8	0.066	$H_2C{=}C{=}O$	$\nu_a(CH_2)$	3155[a]
3101.5	0.018	$H_2C{=}C{=}O$	ν(C=O) + $\rho(CH_2)$ in-plane	
3062.9 3061.6 3059.2	0.288	$H_2C{=}C{=}O$	$\nu_s(CH_2)$	3062[a]
3012.2 3007.3 3006.2 3004.9	*e*	CH_3SH	$\nu_a(CH_3)$	3011.9 3006.4 [b]
2997.9	0.055	CH_3SCH_3	$\nu_a(CH_3)$	2998.2[b]
2972.8 2970.7	0.250	CH_3SCH_3	$\nu_a(CH_3)$	2973.9[b]
2947.6 2938.7 2936.3	0.076	CH_3SH	$\nu_s(CH_3)$	2948.4 2935.9 [b]
2929.1 2924.8 2923.1	0.437	CH_3SCH_3	$\nu_a(CH_3)$	2930.3 2928.4 2925.3 2918.8 [b]
2888.2	0.017	CH_3SCH_3	$\nu_s(CH_3)$	2887.0[b]
2872.6 2868.2 2867.2	0.037	CH_3SCH_3	$\nu_s(CH_3)$	2871.8 2867.6 [b]
2860.4 2858.5	0.016	CH_3SCH_3	$2\delta_a(CH_3)$	2858.1[b]
2839.4	0.015	CH_3SCH_3	$2\delta_a(CH_3)$	2839.4[b]
2137.8 2136.8	4.358	$H_2C{=}C{=}O$	ν(C=O)	2142[a]
2093.6 2091.0 2090.0	0.009	CO	$\nu(^{13}C{\equiv}O)$	2092[c]
2080.4	0.044	$H_2C{=}C{=}O$	$\nu(^{13}C{=}O)$	2085[a]
2049.6	0.004	OCS	ν(C=O)	2049.3[d]
1944.2	0.021	$H_2C{=}C{=}O$	$2\rho(CH_2)$ in-plane	1947[a]
1375.3	0.172	$H_2C{=}C{=}O$	$\delta(CH_2)$	1381[a]
1326.3	0.017	CH_3SH	$\delta_s(CH_3)$	1326.5[b]
1310.4	0.065	CH_3SCH_3	$\delta_s(CH_3)$	1310.8[b]
1068.5	0.085	CH_3SH	$\rho(CH_3)$	1068.2[b]
973.4	0.166	$H_2C{=}C{=}O$	$\rho(CH_2)$ in-plane	974[a]
957.0	*e*	CH_3SH	$\rho(CH_3)$	954.3[b]
799.3	0.003	CH_3SH	δ(CSH)	800.0[b]
703.8	0.015	CH_3SH	ν(C−S)	704.3[b]
567.5	0.333	$H_2C{=}C{=}O$	$\rho(CH_2)$ out-of-plane	591[a]
520.3	0.442	$H_2C{=}C{=}O$	δ(CO) out-of-plane	525[a]
424.7 423.6	0.032	$H_2C{=}C{=}O$	δ(CCO)	438[a]

[a] Reference 28. [b] Reference 33. [c] Reference 27. [d] Reference 34. [e] Could not be measured meaningfully.

band near 1704 cm^{-1} is due to the syn form of **2** occupying a different matrix site.

Otherwise, the IR spectrum that we have recorded is generally in keeping with the results of an earlier study,[36] although there are some differences of detail affecting, for example, the wavenumbers of certain features. It is anticipated satisfactorily with regard to wavenumber and intensity by DFT calculations (see Table 5), the results of which afford a plausible basis for the individual vibrational assignments given.

Photochemistry. Several new IR bands appeared in the IR spectrum when the matrix containing **2** was exposed to broad-band UV−visible light ($200 \leq \lambda \leq 800$ nm), while the bands due to **2** were seen to decay. Table 6 lists the wavenumbers of the bands formed after photolysis for 1 h, together with the proposed assignments of the absorptions. As with **1**, the principal photochemical process results in the formation of ketene, recognizable by the wavenumbers and relative intensities of a family of absorptions near 3155, 3061, 2138, 1375, 973, 567, 520, and 425 cm^{-1} attributable to vibrational fundamentals, as well as weaker features near 3505, 3101, and 1944 cm^{-1} originating in combinations or overtones of the fundamentals.[28] We can also distinguish, in addition to the IR signals associated with ketene but with lower intensities, three other families of signals. One of these, characterized by absorptions near 3010, 2940, 1326, 1068, 957, 799, and 704 cm^{-1}, is easily attributable to CH_3SH.[33,34] A second with absorptions near 2998, 2971, 2925, 2888, 2868, 2859, 2839, and 1310 cm^{-1} can be recognized as belonging to $(CH_3)_2S$, as confirmed by comparison with the spectrum of an Ar matrix doped with an authentic sample of the compound.[33] The third, consisting of just a single weak multiplet centered near 2091 cm^{-1}, we identify with the $\nu(^{13}CO)$ fundamental of CO,[27] the more intense $\nu(^{12}CO)$ counterpart being masked by the intense absorption of ketene at 2138 cm^{-1}.

On the evidence of these results, the main decomposition channel under matrix conditions appears to involve elimination of CH_3SH (eq 6) in a reaction analogous to that disposing chiefly

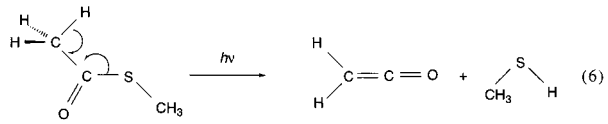

of **1** (eq 3). The presence of $(CH_3)_2S$ and CO molecules may be explained by there being access to an alternative photodissociation pathway (eq 7) that appears to be common to sulfenyl

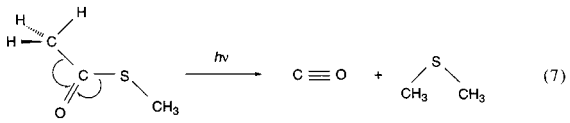

carbonyl compounds.[1−3] By contrast with the behavior of **1**, however, there is no sign to suggest the formation of OCS and C_2H_6 (cf. eq 4).

(iii) $CH_3C(O)SC(O)CH_3$, 3. The structures of gaseous and crystalline diacetyl sulfide, $CH_3C(O)SC(O)CH_3$ (**3**), have been determined recently.[9] Hence, it is found that the molecule has a planar heavy-atom skeleton with the [sp,ap] conformation in both the gas and solid phases. The IR spectrum of the molecule isolated in an Ar matrix has also been shown[9] to be consistent with the [sp,ap] conformation, with the results wholly in keeping with the predictions of theoretical calculations. Here, we describe the outcome of further experiments designed to explore the photochemistry of **3** isolated in an Ar, a N_2, or a CO-doped Ar matrix. Inspection of the spectra of the irradiated matrixes showed that the photoproducts and the rates of their formation were almost the same in the three different matrix environments, with only minor exceptions to be discussed later. There were no signals in the IR spectra of the different matrixes that could be attributed to the formation of another conformer of **3** under the action of broad-band UV−visible light. Instead, a host of new bands appeared on photolysis, with the wavenumbers and intensities listed in Table 7. To assign the various bands, and so identify their carriers, we have taken into account (i) their distinctive behaviors as a function of irradiation time, and (ii) the locations and relative intensities of all of the bands associated with a particular compound. Figures 4−6, 8, and 9 depict plots of the integrated intensities of the more prominent bands displayed by an Ar matrix; these are given as a function of irradiation times ranging from 1 to 240 min. Figure 4 illustrates

TABLE 7: Wavenumbers, Intensities, and Assignments of the IR Absorptions Appearing after 120 min of Broad-Band Photolysis of $CH_3C(O)SC(O)CH_3$ Isolated in an Ar, N_2, or CO-Doped Ar Matrix

Ar matrix		N_2 matrix	Ar + 5% CO matrix	assignment		wavenumber reported previously
ν [cm^{-1}]	I	ν [cm^{-1}]	ν [cm^{-1}]	molecule	vibrational mode	
3509.4 3504.7	0.049	3512.0	3504.5	$H_2C{=}C{=}O$	ν(C=O) + $\delta(CH_2)$	3513[a]
3255.5	0.122	3255.7	3257.5	$H_2C{=}C{=}O$	ν(C=O) + ν(C−C)	3255[a]
3157.8 3154.8	0.274	3161.3	3155.1	$H_2C{=}C{=}O$	$\nu_a(CH_2)$	3155[a]
3102.8	0.053	3108.9	3101.0	$H_2C{=}C{=}O$	ν(C=O) + $\rho(CH_2)$ in-plane	
3067.3 3061.6 3058.6 3055.6 3049.8 3045.3 3040.6	0.554	3063.7 3062.0 3059.4 3058.0	3060.9	$H_2C{=}C{=}O$	$\nu_s(CH_2)$	3062[a]
2970.7	0.052	2970.2	2970.9			
2947.2	0.023	2945.9	2946.3	CH_3SH	$\nu_a(CH_3)$	2948.4[b]
2685.6	0.040					
2624.9	0.007	2621.5 2615.7	2622.1		ν(SH)	
2605.4 2590.8	0.018	2598.5 2594.2	2604.5 2587.6		ν(SH)	
2570.2 2567.8	0.125	2582.8 2578.6	2567.2		ν(SH)	
2560.7 2556.4	0.002	2561.0			ν(SH)	
2547.8	0.008	2552.1			ν(SH)	
2532.9	0.034	2545.5 2543.4 2540.4	2532.2	$CH_3C(O)SH$	ν(SH)	
2144.2 2140.3 2139.9 2137.8 2137.8	12.852	2145.8 2143.5 2140.9 2139.4 2138.5 2136.9 2135.1		$H_2C{=}C{=}O$	ν(C=O)	2142[a]
2082.5	0.129	2084.0	2082.3	$H_2C{=}C{=}O$	$\nu(^{13}C{=}O)$	2085[a]
2049.6	0.227	2053.2	2049.7	OCS	ν(C=O)	2049.3[c]
1944.2	0.071	1952.3	1944.2	$H_2C{=}C{=}O$	2$\rho(CH_2)$ in-plane	1947[a]
			1863.3 1861.9	HCO	ν(C=O)	1863[d]
1718.3	0.275	1717.5	1719.0[g]	$CH_3C(O)SH$	ν(C=O)	1722.5[e]
1697.5	0.016	1697.3	1698.9	$CH_3C(O)SCH_3$	ν(C=O)	1709.3 1701.6 1695.2 1683.5 1665.5 [e]
1527.2 1512.2	0.107	1525.9 1514.9	1524.5 1514.3			
1446.3	0.018	1447.9	1446.6			
1385.9 1378.5 1376.8 1375.3	0.317	1381.3 1379.4 1378.4	1377.4 1374.4	$H_2C{=}C{=}O$	$\delta(CH_2)$	1381[a]
1355.3	0.03			$CH_3C(O)SH$	$\delta_s(CH_3)$	1355.2[e]
1327.6	0.007	1329.7	1327.2	CH_3SH	$\delta_s(CH_3)$	1326.5[b]
1304.6	0.038	1305.3	1304.1	CH_4	$\delta_s(CH_3)$	1307.7[f]
1282.9 1276.1 1272.9	0.010		1282.0 1275.6			
1129.7	*g*	1132.5	1130.9	$H_2C{=}C{=}O$	$\rho(CH_2)$ out-of-plane + δ(CO) out-of-plane	1126[a]
1121.0	*g*			$H_2C{=}C{=}O$	ν(C−C)	1115[a]
1069.7	0.013	1079.2 1076.0 1070.1	1069.0	CH_3SH	$\rho(CH_3)$	1068.3[b]
992.6	0.094	992.9	992.7			
973.4	0.086	977.3	973.5	$H_2C{=}C{=}O$	$\rho(CH_2)$ in-plane	974[a]
522.9 519.6	0.736	523.2	522.1	$H_2C{=}C{=}O$	δ(CO) out-of-plane	525[a]

[a] Reference 28. [b] Reference 33. [c] Reference 34. [d] Reference 38. [e] This work. [f] Reference 35. [g] Could not be measured meaningfully.

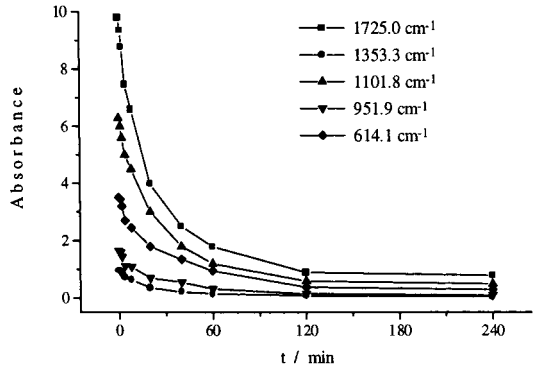

Figure 4. Plot of the intensities of the bands assigned to $CH_3C(O)SC(O)CH_3$ in the IR spectrum of an Ar matrix initially containing diacetyl sulfide vs irradiation time.

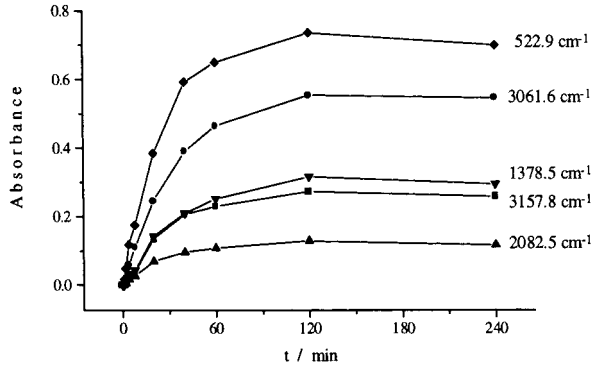

Figure 5. Plot of the intensities of the bands assigned to $CH_2{=}C{=}O$ in the IR spectrum of an Ar matrix initially containing diacetyl sulfide vs irradiation time.

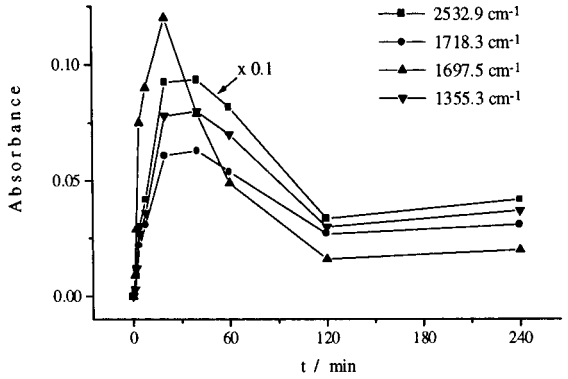

Figure 6. Plot of the intensities of the bands assigned to $CH_3C(O)SH$ (2532.9, 1718.3, and 1355.3 cm^{-1}) and $CH_3C(O)SCH_3$ (1697.5 cm^{-1}) in the IR spectrum of an Ar matrix initially containing diacetyl sulfide vs irradiation time.

the decay with time of the most intense absorptions associated with **3**, which occur near 1725, 1353, 1102, 952, and 614 cm^{-1}. The intensities of the absorptions that develop near 3158, 3062, 2082, 1378, and 523 cm^{-1} (see Figure 5) grow continuously on photolysis, tending asymptotically to limiting values. These features clearly arise from the photostable ketene molecule,[28] the most intense IR band of which, occurring near 2138 cm^{-1}, also follows the same pattern of growth. Figure 6 shows the corresponding behavior of a set of bands centered near 2533, 1718, 1697, and 1355 cm^{-1} that first grow and then decay on continued photolysis. Three of them—those at 2533, 1718, and 1355 cm^{-1}—present the same pattern, suggesting either that they are associated with a single product or that they arise from different products formed in a common photochemical channel.

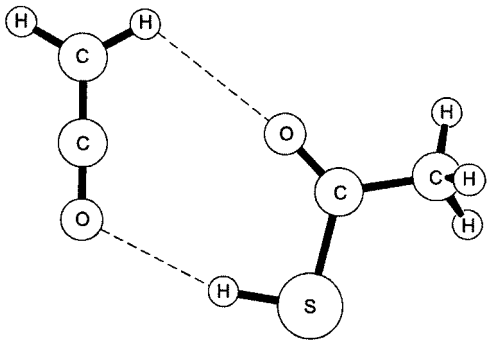

Figure 7. B3LYP/6-31+G* geometry of the $CH_3C(O)SH\cdots H_2CCO$ adduct.

On the other hand, the band near 1697 cm^{-1} follows a different pattern so must come from another source (which see).

The absorptions at ca. 1718 and 1355 cm^{-1} can be assigned, respectively, to the ν(CO) and $\delta(CH_3)$ fundamentals of $CH_3C(O)SH$, **1**, in keeping with the results described earlier (see Table 1). The presence of this photoproduct can be readily explained by the following decomposition reaction (eq 8, cf. eqs 3 and 6).

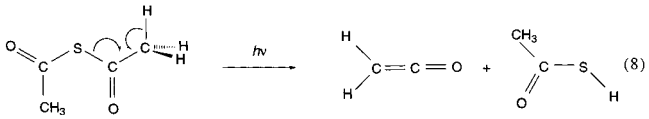

The transition at ca. 2533 cm^{-1} must then be supposed to represent the ν(SH) fundamental of **1** but perturbed with respect to the free molecule. Attempts to find other bands of $CH_3C(O)SH$ in the IR spectrum of the irradiated matrix failed, presumably because they were masked by the absorptions of the parent compound (e.g., those near 1143 and 615 cm^{-1}) or were too weak to be detected under the conditions of these experiments.

The ν(SH) wavenumber of **1**, allied to the complicated multiplet patterns displayed by some of the ketene bands (e.g., those at ca. 3056, 2139, and 1378 cm^{-1}), gives us reason to believe that the decomposition described by eq 8 leads to a loose complex between the two products, which are necessarily confined at the site of their formation by the rigidity of the Ar matrix. The shift of approximately 70 cm^{-1} and the marked intensification of the ν(SH) absorption with respect to the isolated molecule **1** certainly support this view. Moreover, DFT calculations predict for the system $CH_3C(O)SH\cdots H_2CCO$ a stabilized structure interacting through two different hydrogen bonds, one between the H of the S−H group of **1** and the carbonyl O of the ketene and the other between the carbonyl O of **1** and one of the H atoms of the ketene (see Figure 7).[37]

The IR band occurring near 1697 cm^{-1} may be attributed to the ν(CO) fundamental of $CH_3C(O)SCH_3$, **2**. As in the case of **1**, however, the other absorptions of **2** are obscured by stronger absorptions due to either the diacetyl sulfide precursor or ketene (see ref 9 and Tables 5 and 7). With the identification of **2** as a product comes the presumption that it results from the elimination of CO from **3** in accordance with eq 9. No IR feature

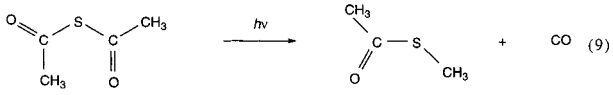

could be positively ascribed in fact to free CO, but this we believe to be due either to masking by the intense ν(CO)

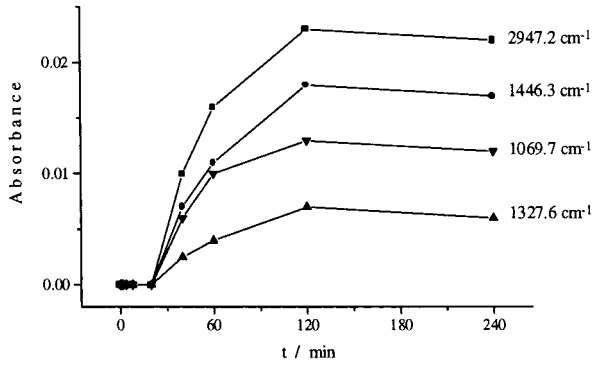

Figure 8. Plot of the intensities of the bands assigned to CH_3SH in the IR spectrum of an Ar matrix initially containing diacetyl sulfide vs irradiation time.

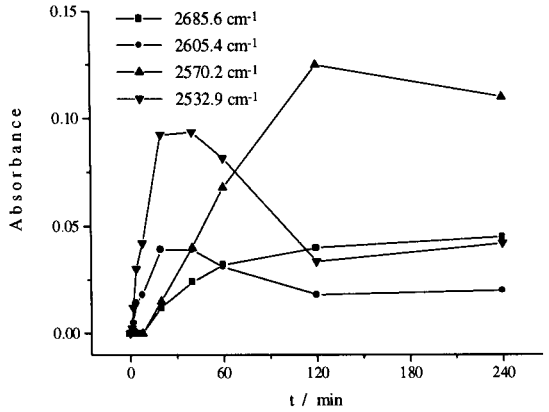

Figure 9. Plot of the ν(SH) region in the IR spectrum of an Ar matrix initially containing diacetyl sulfide vs irradiation time.

multiplet of ketene (which see) or to having insufficient intensity (in the case of the ^{13}CO satellite expected near 2091 cm^{-1}).

Figure 8 shows the behavior of a set of bands near 2947, 1446, 1328, and 1070 cm^{-1}, which appear after 20 min of broad-band UV−visible photolysis. There can be no doubt that these bands signal the formation of CH_3SH, a conclusion endorsed by comparison with the IR spectrum of an authentic sample of the compound isolated in an Ar matrix.[33,34] However, the region of the spectrum corresponding to ν(SH) modes (2500−2700 cm^{-1}) presents a rather complicated pattern. At least six absorptions appear in this region with intensities that differ as a function of irradiation time, as illustrated in Figure 9. In addition to the loose $CH_3C(O)SH\cdots H_2CCO$ adduct already described, CH_3SH must be responsible for at least some of these, whether in the form of the free molecule or a loose adduct, for example, $CH_3SH\cdots H_2CCO$. At the same time, the presence of H_2S cannot be excluded. On the other hand, signals corresponding to OCS (near 2050 cm^{-1}) and to CH_4 (near 1305 cm^{-1}) could be discerned in the spectrum of the irradiated matrix. All of these species, that is, CH_3SH, OCS, and CH_4, are consistent with the photodecay of the two primary products **1** and **2** (see eqs 8 and 9) via channels such as those represented, for example, by eqs 4 and 6.

There is a band occurring at 1862 cm^{-1}, which appears only on photolysis of the CO-doped Ar matrix. This we assign to the HCO radical on the basis of earlier studies carried out by Milligan and Jacox,[38] which found that Ar matrixes containing this species are characterized by strong absorption at 1863 cm^{-1}. The formation of HCO is significant in its implication that C−H or S−H bonds are being ruptured to release hydrogen atoms[39] in one among the various events that are induced by photolysis of an Ar matrix doped with **3**.

Conclusions

The matrix photochemistries of each of the three methyl sulfenyl carbonyl compounds, $CH_3C(O)SH$ (**1**), $CH_3C(O)SCH_3$ (**2**), and $CH_3C(O)SC(O)CH_3$ (**3**), are characterized by the formation of ketene as a major product, together with the appropriate thiol RSH (where R = H, CH_3, and CH_3CO, respectively). These results contrast with the preferred modes of photodecomposition of matrix-isolated sulfenyl carbonyl compounds, XC(O)SY where X is *not* a methyl group, namely, elimination of CO and OCS as in eqs 10 and 11.[1−3]

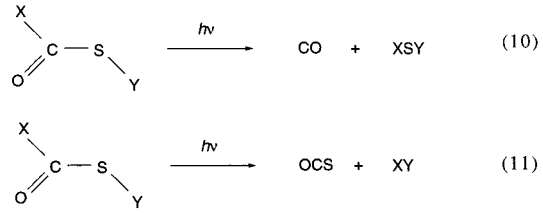

The difference between these two processes and the one leading to the formation of ketene must have its origin in the photolability of the acetyl group. If the methyl is replaced by a perfluoromethyl group, as in the case of $CF_3C(O)SH$, photochemical decomposition reverts to the pathway described by eq 10.[26]

Although the detachment of a hydrogen atom from a methyl group is the dominant process brought about by photolysis of the matrix-isolated $CH_3C(O)SX$ compounds, it is not the exclusive pathway, with photodecomposition proceeding additionally and simultaneously by reactions of the types represented by eqs 10 and 11. Some of the products of the various reactions are themselves photolabile. Such is the case, for example, with $CH_3C(O)SH$ and $CH_3C(O)SCH_3$, which feature as intermediates contributing to the unusually rich matrix photochemistry of diacetyl sulfide.

Use of the B3LYP/6-31+G* method to estimate the reaction energies, ΔE, for the three possible decomposition routes open to an acetyl sulfenyl compound $CH_3C(O)SY$ (eq 12) gives the

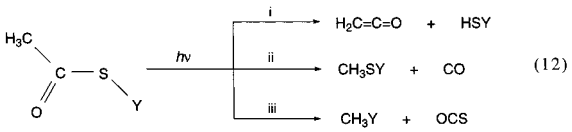

following results (listed in kcal mol^{-1} in the order Y = H, CH_3, and $C(O)SCH_3$): (i) formation of ketene + HSY, +31.6, +35.1, and +26.9; (ii) formation of CO + CH_3SY, +16.6, +18.3, and +8.4; (iii) formation of OCS + CH_3Y, −10.8, −6.1, and −8.0. Hence, only the third reaction, which plays a relatively minor role, appears to be exothermic. More significant, however, is the finding that no one reaction has an overwhelming thermodynamic advantage over the others, although we cannot judge the magnitudes of the kinetic barriers.

The formation of ketene from an acetyl derivative is by no means new. A reaction similar to that in eq 12i is well-known as a secondary channel (eq 13i) competing with the primary

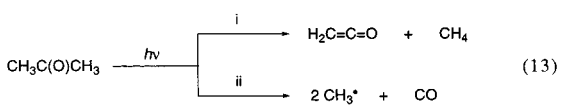

channel (eq 13ii) on UV photolysis of acetone vapor,[40] albeit a channel that can be exploited for the preparation of ketene.[41] Electron bombardment of acetone followed by matrix isolation

of the products also gives ketene as a minor product, which is probably derived, however, from the acetone cation.[42] By contrast, irradiation of matrix-isolated $CH_3C(O)Cl$ at wavelengths >270 nm is reported[43] to form almost exclusively the complex $H_2CCO{\cdot}HCl$. Studies of the photodecomposition of gaseous acetone suggest[40] that there are two possible primary events the relative probability of which varies with the wavelength of the photolyzing radiation, as well as the other conditions. One involves rupture of the C−C bond to form acetyl and methyl radicals (eq 14i), and the other involves rupture of

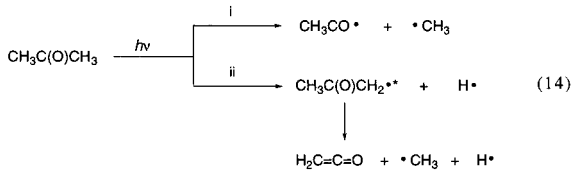

(14)

a C−H bond to form the acetonyl radical, $CH_3C(O)CH_2^{\bullet}$, and H atoms (eq 14ii). In the case of the second process, the acetonyl radical is expected to be vibrationally excited and to carry an excess of energy sufficient to enable further dissociation to occur, giving ketene, a methyl radical, and a second H atom. The ability of matrix conditions to favor the formation of ketene may then depend on the comparative mobility of H atoms in solid noble gas matrixes[44] allowing them to escape the matrix cage and so prevent the regeneration of the precursor. By contrast, the $CH_3CO^{\bullet}$ and $CH_3^{\bullet}$ radicals formed in the first process are likely to be entrained within the matrix cage so that recombination is the dominant outcome. We believe that the predominance of ketene and HSY as products in the matrix photochemistry of the acetyl sulfenyl compounds $CH_3C(O)SY$ (eq 12i) hinges on this feature (with the radical $^{\bullet}CH_2C(O)SY$ being formed in place of $CH_3C(O)CH_2^{\bullet}$), although the ability of other components of the matrix, for example, $CH_3^{\bullet}$ or $CH_3S^{\bullet}$, to scavenge the H atoms may also play a significant part.

In addition to the identification of the various decay products and the different decomposition pathways leading to them, the present study has also been concerned with the conformational properties of thioacetic acid and its methyl ester. Both the experimental and theoretical results agree that the vapor of the parent acid at ambient temperatures is composed of a mixture of the syn and anti conformers, with the syn form being more stable than the anti one by 1.8−2.4 kcal mol^{-1}. Photochemical interconversion provides an effective means of characterizing the different matrix-isolated conformers by their IR spectra. By contrast, the low electron-scattering cross-section of X···H atom pairs (X = H, C, or O) causes the electron-diffraction pattern to be relatively uninformative as regards the conformational makeup of the vapor. In the case of methyl thioacetate, however, the IR spectra of the syn and anti forms are likely to differ but little, and apart from a single band, which may be due to the ν(CO) fundamental, there has been no definite and distinctive sign of the less stable anti form.

Acknowledgment. The authors acknowledge with thanks a British Council-Fundación Antorchas award for British-Argentine cooperation and a Jesus College (Oxford) grant. C.O.D.V. and R.M.R. thank Consejo Nacional de Investigaciones Científicas y Técnicas (CONICET) (Grant PIP 4695), Comisión de Investigaciones Científicas de la Provincia de Buenos Aires (CIC), and Facultad de Ciencias Exactas, Universidad Nacional de La Plata for financial support. R.M.R. also acknowledges with gratitude a Fundación Antorchas grant. In addition, A.J.D. is indebted to the EPSRC for support, including the purchase of equipment.

References and Notes

(1) Romano, R. M.; Della Védova, C. O.; Downs, A. J.; Greene, T. M. *J. Am. Chem. Soc.* **2001**, *123*, 5794.
(2) Willner, H. *Z. Naturforsch., B: Anorg. Chem., Org. Chem.* **1984**, *39*, 314.
(3) Della Védova, C. O.; Mack, H.-G. *Inorg. Chem.* **1993**, *32*, 948.
(4) Mack, H.-G.; Oberhammer, H.; Della Védova, C. O. *J. Mol. Struct.* **1992**, *265*, 347.
(5) Mack, H.-G.; Oberhammer, H.; Della Védova, C. O. *J. Phys. Chem.* **1991**, *95*, 4238.
(6) Della Védova, C. O.; Cutin, E. H.; Jubert, A. H.; Varetti, E. L.; Aymonino, P. J. *Can. J. Spectrosc.* **1984**, *29*, 130.
(7) Della Védova, C. O. *J. Raman Spectrosc.* **1989**, *20*, 729.
(8) Romano, R. M.; Della Védova, C. O.; Downs, A. J. Unpublished results.
(9) Romano, R. M.; Della Védova, C. O.; Downs, A. J.; Oberhammer, H.; Parsons, S. *J. Am. Chem. Soc.* **2001**, *123*, 12623.
(10) Gordy, W. *J. Chem. Phys.* **1946**, *14*, 560.
(11) Gobatto, K. I.; Della Védova, C. O.; Mack, H.-G.; Oberhammer, H. *Inorg. Chem.* **1996**, *35*, 6152.
(12) Bonner, W. A. *J. Am. Chem. Soc.* **1950**, *72*, 4270.
(13) Fortunato, B.; Giorgini, M. G.; Mirone, P. *J. Mol. Struct.* **1975**, *25*, 237.
(14) Almond, M. J.; Downs, A. J. *Adv. Spectrosc.* **1989**, *17*, 1. Dunkin, I. R. *Matrix-Isolation Techniques: A Practical Approach*; Oxford University Press: New York, 1998.
(15) Perutz, R. N.; Turner J. J. *J. Chem. Soc., Faraday Trans. 2* **1973**, *69*, 452.
(16) Frisch, M. J.; Trucks, G. W.; Schlegel, H. B.; Scuseria, G. E.; Robb, M. A.; Cheeseman, J. R.; Zakrzewski, V. G.; Montgomery, J. A., Jr.; Stratmann, R. E.; Burant, J. C.; Dapprich, S.; Millam, J. M.; Daniels, A. D.; Kudin, K. N.; Strain, M. C.; Farkas, O.; Tomasi, J.; Barone, V.; Cossi, M.; Cammi, R.; Mennucci, B.; Pomelli, C.; Adamo, C.; Clifford, S.; Ochterski, J.; Petersson, G. A.; Ayala, P. Y.; Cui, Q.; Morokuma, K.; Malick, D. K.; Rabuck, A. D.; Raghavachari, K.; Foresman, J. B.; Cioslowski, J.; Ortiz, J. V.; Stefanov, B. B.; Liu, G.; Liashenko, A.; Piskorz, P.; Komaromi, I.; Gomperts, R.; Martin, R. L.; Fox, D. J.; Keith, T.; Al-Laham, M. A.; Peng, C. Y.; Nanayakkara, A.; Gonzalez, C.; Challacombe, M.; Gill, P. M. W.; Johnson, B. G.; Chen, W.; Wong, M. W.; Andres, J. L.; Head-Gordon, M.; Replogle, E. S.; Pople, J. A. *Gaussian 98*, revision A.7; Gaussian, Inc.: Pittsburgh, PA, 1998.
(17) Randhawa, H. S.; Walter, W.; Meese, C. O. *J. Mol. Struct.* **1977**, *37*, 187.
(18) Sheppard, N. *Trans. Faraday Soc.* **1949**, *45*, 693.
(19) Mecke, R.; Spiesecke, H. *Chem. Ber.* **1956**, *89*, 1110.
(20) Sjöberg, B. *Acta Chem. Scand.* **1957**, *11*, 945.
(21) Engler, G. R.; Gattow, G. *Z. Anorg. Allg. Chem.* **1972**, *388*, 78.
(22) Randhawa, H. S.; Rao, C. N. R. *J. Mol. Struct.* **1974**, *21*, 123.
(23) Nyquist, R. A.; Potts, W. J. *Spectrochim. Acta* **1959**, *15*, 514.
(24) Crowder, G. A. *Appl. Spectrosc.* **1972**, *26*, 486.
(25) Noe, E. A. *J. Am. Chem. Soc.* **1977**, *99*, 2803.
(26) Ulic, S. E.; Gobbato, K. I.; Della Védova, C. O. *J. Mol. Struct.* **1997**, *407*, 171.
(27) Dubost, H. *Chem. Phys.* **1976**, *12*, 139.
(28) Moore, C. B.; Pimentel, G. C. *J. Chem. Phys.* **1963**, *38*, 2816.
(29) Bandow, H.; Akimoto, H. *J. Phys. Chem.* **1985**, *89*, 845.
(30) Barnes, A. J.; Howells, J. D. R. *J. Chem. Soc., Faraday Trans. 2* **1972**, *68*, 729.
(31) Lundell, J.; Nordquist, E.; Räsänen, M. *J. Mol. Struct.* **1997**, *416*, 235.
(32) Barnes, A. J.; Hallam, H. E.; Howells, J. D. R. *J. Mol. Struct.* **1974**, *23*, 463.
(33) Romano, R. M.; Della Védova, C. O.; Downs, A. J. Unpublished results.
(34) Hawkins, M.; Almond, M. J.; Downs, A. J. *J. Phys. Chem.* **1985**, *89*, 3326.
(35) Cabana, A.; Savitsky, G. B.; Hornig, D. F. *J. Chem. Phys.* **1963**, *39*, 2942. Frayer, F. H.; Ewing, G. E. *J. Chem. Phys.* **1968**, *48*, 781. Chamberland, A.; Belzile, R.; Cabana, A. *Can. J. Chem.* **1970**, *48*, 1129.
(36) Smolders, A.; Maes, G.; Zeegers-Huyskens, T. H. *J. Mol. Struct.* **1988**, *172*, 23.
(37) Romano, R. M. Unpublished results.
(38) Milligan, D. E.; Jacox, M. E. *J. Chem. Phys.* **1969**, *51*, 277.
(39) Perutz, R. N. *Chem. Rev.* **1985**, *85*, 77.
(40) Lightfoot, P. D.; Kirwan, S. P.; Pilling, M. J. *J. Phys. Chem.* **1988**, *92*, 4938.
(41) Ferris, R. C.; Haynes, W. S. *J. Am. Chem. Soc.* **1950**, *72*, 893.
(42) Zhang, X. K.; Parnis, J. M.; Lewars, E. G.; March, R. E. *Can. J. Chem.* **1997**, *75*, 276.
(43) Kogure, N.; Ono, T.; Suzuki, E.; Watari, F. *J. Mol. Struct.* **1993**, *296*, 1.
(44) See, for example: Bondybey, V. E.; Räsänen, M.; Lammers, A. *Annu. Rep. Prog. Chem., Sect. C* **1999**, *95*, 331.